Journal of Dental Sciences 20 (2025) 560–568

Available online at www.sciencedirect.com

ScienceDirect

journal homepage: www.e-jds.com

Original Article

Periodontal ligament fibroblasts utilize isoprenoid intermediate farnesyl diphosphate for maintaining osteo/cementogenic differentiation abilities

Xiuting Wang [a], Shigeki Suzuki [a*], Hang Yuan [a,b], Shizu Hirata-Tsuchiya [c], Rahmad Rifqi Fahreza [a], Eiji Nemoto [a], Hideki Shiba [c], Satoru Yamada [a]

[a] *Department of Periodontology and Endodontology, Tohoku University Graduate School of Dentistry, Sendai, Japan*
[b] *Tenth People's Hospital of Tongji University Department of Stomatology, Shanghai, China*
[c] *Department of Biological Endodontics, Graduate School of Biomedical and Health Sciences, Hiroshima University, Hiroshima, Japan*

Received 4 April 2024; Final revision received 26 April 2024
Available online 3 May 2024

KEYWORDS
Periodontal tissue regeneration;
Energy metabolism;
Isoprenoid synthesis;
Periodontal ligament fibroblasts;
Peroxisome proliferator-activated receptor γ

Abstract *Background/purpose:* Peroxisome proliferator-activated receptor γ (PPARγ) is a major transcription factor of energy metabolism-associated genes, and three PPARγ isoforms have been identified in periodontal tissues and cells. When energy metabolism homeostasis is affected by PPARγ downregulation in periodontal ligament fibroblasts (PDLFs), osteo/cementogenic abilities are markedly lost. Herein, we investigated whether PPARγ agonists promote periodontal tissue regeneration, and which PPARγ isoforms and metabolic pathways are indispensable for osteo/cementogenic abilities.

Materials and methods: A PPARγ agonist was locally administered to regenerate murine periodontal tissue. The distinct functions of the PPARγ isoforms in PDLFs were assessed using an overexpression strategy. Candidate metabolic processes were searched using gene ontology analysis of PPARγ-knockdown PDLFs. *In vitro* differentiation assays were performed to evaluate the effects of farnesyl diphosphate (FPP) and geranylgeranyl diphosphate (GGPP), two major isoprenoid intermediates.

Results: PPARγ agonists accelerated periodontal tissue regeneration. Full-length PPARγ overexpression specifically enhanced the osteo/cementogenic differentiation of PPARγ agonist–induced PDLFs. The isoprenoid metabolic process was the top-ranked downregulated metabolism-associated pathway following PPARγ knockdown; FPP and GGPP enhanced and

* Corresponding author. Department of Periodontology and Endodontology, Tohoku University Graduate School of Dentistry, 4-1, Seiryo-machi, Aoba-ku, Sendai 980-8575, Japan.
E-mail address: shigeki.suzuki.b1@tohoku.ac.jp (S. Suzuki).

https://doi.org/10.1016/j.jds.2024.04.025

suppressed PDLFs' differentiation, respectively. Gene expression analysis of human clinical periodontal tissues revealed that *osteocalcin* correlated with *farnesyl pyrophosphate synthetase* (*FDPS*), which catalyzes FPP production, but not with two FPP conversion enzymes: *geranylgeranyl diphosphate synthase 1* (*GGPS1*) or *farnesyl diphosphate farnesyltransferase 1* (*FDFT1*).

Conclusion: Preferable PPARγ agonistic actions depend on the full-length PPARγ isoform. FPP increased PDLFs' osteo/cementogenic abilities. Therefore, administering FPP and precisely controlling FDPS, GGPS1, and FDFT1 activities could be a novel strategy for accelerating periodontal tissue regeneration.

Introduction

Fibroblastic cells in periodontal ligament tissue (periodontal ligament fibroblasts, PDLFs) possess stem cell—like properties and, thus, can differentiate into osteo/cementogenic cells.[1—5] Inhibition of Wingless, the *Drosophila melanogaster* segment-polarity gene, and integrase-1, the vertebrate homologue (Wnt) secretion, such as Wnt3a, a key inducer of osteogenesis and cementogenesis, in murine PDLFs leads to a higher width of periodontal ligament tissue and suppresses the expression of osteogenic markers in periodontal ligament tissue.[6] Therefore, osteo/cementogenic abilities of PDLFs are indispensable for maintaining periodontal tissue homeostasis. During periodontal regeneration, PDLFs proliferate and migrate from the remaining periodontal ligament tissue to the surgically disinfected space and reconstruct the physiological periodontal tissue composed of cementum, alveolar bone, and periodontal ligament tissue.[7]

PDLFs utilize energy metabolic processes to maintain osteo/cementogenic differentiation abilities.[8] Knockdown of peroxisome proliferator-activated receptor γ (PPARγ), a key transcription factor for genes involved in energy metabolic pathways, in PDLFs results in a marked reduction in the expression of osteo/cementogenic-related and extracellular matrix (ECM)-related genes. Moreover, thiazolidinedione compounds (TZDs), chemical agonists of PPARγ, such as rosiglitazone and troglitazone, enhance the osteo/cementogenic abilities *in vitro*.[8] Periodontal tissue/cells express three isoforms of PPARγ: a full-length PPARγ and two partially deleted isoforms, ubiquitous isoform of PPARγ (PPARγ-UBI) and periodontal isoform of PPARγ (PPARγ-PDL).[9] PPARγ-UBI was previously identified in adipocytes, and PPARγ-PDL was newly identified as a PDL-specific isoform.[9,10] Local application of procyanidin B2, a PPARγ ligand, into the periodontal tissue of ligature-induced periodontitis mice prevents alveolar bone loss.[9] Mechanistically, PDLFs treated with procyanidin B2 exhibit suppressed expression of PPARγ-UBI, which stabilizes the nuclear factor kB (NF-kB) p65 and the expression of genes encoding pro-inflammatory cytokines. PPARγ isoform-dependent functions have been identified; however, the distinct functions of PPARγ isoforms in osteo/cementogenic differentiation remain unclear.

PPARγ is a key modulator of energy metabolism, such as lipid and glucose metabolism;[11] acetyl coenzyme A (acetyl-CoA) is a central coordinator for lipid and glucose metabolism.[12] However, which metabolic pathways and intermediates contribute to maintaining the osteo/cementogenic abilities of PDLFs remain unclear.

In the present study, we assessed the effects of TZDs on periodontal tissue regeneration. Next, the osteo/cementogenic abilities of the three PPARγ isoforms in PDLFs were explored. Subsequently, the isoprenoid metabolic pathway was identified as the most severely downregulated metabolic pathway in PPARγ-knockdown PDLFs. Isoprenoid synthesis originates from the mevalonate pathway, which starts with the conversion of 3-hydroxy-3-methylglutaryl-CoA to mevalonic acid, and then synthesizes intermediates such as farnesyl diphosphate (FPP) and geranylgeranyl diphosphate (GGPP) by the condensation reaction of isopentenyl diphosphate (IPP) and dimethylallyl diphosphate (DMAPP). Therefore, FPP and GGPP were used to identify the key intermediates for osteo/cementogenic abilities.

Materials and methods

Reagents

Rosiglitazone (R2408), FPP ammonium salt (F6892), and GGPP ammonium salt (G6025) were obtained from Sigma-Aldrich (St. Louis, MO, USA). Troglitazone (209—19481) was purchased from FUJIFILM Wako Pure Chemical Corporation (Osaka, Japan).

Experimental animals

All experimental procedures conformed to the "Regulations for Animal Experiments and Related Activities at Tohoku University" and were reviewed by the Institutional Laboratory Animal Care and Use Committee of Tohoku University and approved by the President of the University (Permit No. 2020DnA-044-06). Eleven-week-old male C57BL6/J mice (specific pathogen-free grade) were purchased from CLEA Japan, Inc. The mice were allowed to adapt to the new environment for one week before the experiments. The mice were anesthetized, and silk ligatures (Elp Sterile Blade Silk, Black, 5—0, Akiyama Medical MFG, Tokyo, Japan) were tied around the left second maxillary molar for 14 days. After the 14-day periodontal inflammation period,

rosiglitazone (1.2 mg/kg) dissolved in solvent (50% DPBS, 40% PEG300, 5% Tween 80, 5% DMSO) was locally applied into the mesial and distal sides of the left second maxillary molars every other day for 14 days. The mice in the control group were administered the same amount of solvent at the same frequency. The right maxillae of the rosiglitazone and solvent-treated control groups were not treated throughout the experimental period.

Micro-computed tomography

Micro-computed tomography (μCT) was conducted as previously described.[9,13] The vertical distances from the cemento-enamel junction to the alveolar bone crest at the mesial and distal roots of the second maxillary molars were measured and added. This sum was used to quantitatively compare bone regeneration levels in the periodontal regeneration stage.

Histology

The maxilla samples used for μCT analysis were decalcified using ethylenediaminetetraacetic acid at 4 °C for 2 weeks. Masson's trichrome staining was performed on 5 μm-thick paraffin sections as previously described.[14–16]

Cell culture and stable cell line generation

Human PDLFs were purchased from Lonza Inc. (Walkersville, MD, USA) and maintained in low-glucose Dulbecco's modified Eagle medium (DMEM; Thermo Fisher Scientific, Carlsbad, CA, USA) supplemented with 100 units/mL of penicillin, 100 μg/mL of streptomycin, and 10% fetal bovine system. PDLFs were cultivated at 37 °C under humidified atmospheric conditions (5% CO_2 and 95% air). PDLFs stably expressing the full-length (PPARγ), PPARγ-UBI, and PPARγ-PDL were generated as previously described.[9] For inducing osteo/cementogenic differentiation, PDLFs were cultured in an induction medium (low-glucose DMEM with 10% FBS, ascorbic acid (100 μg/mL), and β-glycerophosphate (10 mM)) in the presence or absence of troglitazone or rosiglitazone for 12 days.

Alkaline phosphatase activity

Alkaline phosphatase (ALP) activity was measured as previously described[17] and normalized to the cell numbers obtained from a parallel cell culture.[18]

Alizarin red S staining

Alizarin red S staining and the average intensity calculations were performed as previously described.[19]

RNA-seq data processing

The RNA-seq dataset deposited in NCBI's Gene Expression Omnibus (GEO, accession number: GSE178607) was processed as previously described.[8,20] Subsequently, gene ontology analyses of enhanced biological processes of the PDLFs transfected with control siRNA relative to the cells transfected with siRNA for *PPARγ* were conducted to identify the pathways suppressed by *PPARγ* knockdown.

Quantitative reverse transcription polymerase chain reaction

Total RNA purification, cDNA preparation, and quantitative reverse transcription polymerase chain reaction (qPCR) were conducted as previously described.[21–23] *Osteocalcin* (*OCN*) and *collagen type I alpha 1 chain* (*COL1A1*) expression analyses were conducted previously.[9] *Hypoxanthine phosphoribosyltransferase 1* (*HPRT*) was used as the internal reference control. The qPCR primer sequences used for the target genes are listed in Table 1.

Immunohistochemical analyses

Immunostaining was performed on 5-μm thick paraffin sections. The fixed maxillae of 1.5-month-old male mice were decalcified and embedded in paraffin as described above. The sections were stained with Alexa Fluor™ 488 Tyramide SuperBoost™ Kit (B40922, Thermo Fisher Scientific) according to the manufacturer's instructions. The sections were incubated with rabbit IgG (DA1E, Cell Signaling Technologies, Danvers, MA, final concentration 10 μg/mL), rabbit anti-farnesyl diphosphate farnesyltransferase 1

Table 1 Primer pairs used in this study.

Primer name	Species	Direction	Sequence
AKR1C3	Human	forward	ATCCGAAGCAAGATTGCAGA
		reverse	GGACCAACTCTGGTCGATGA
ALDH3A2	Human	forward	GGCAAAGCTTCTCCCTCAGT
		reverse	CCATGACAATTTTGCCAACC
AKR1C1	Human	forward	CAGCCTTGGAAAGGTCACTG
		reverse	TGGGATCACTTCCTCACCTG
SDC3	Human	forward	GGGCTACTTCGAGCAGGAGT
		reverse	GAGGGGAGCTCTTCAAATGG
FDPS	Human	forward	AGGGCAATGTGGATCTTGTC
		reverse	GAAAGAACTCCCCCATCTCC
GGPS1	Human	forward	TTGGCTGAAAGTTCCAGAGG
		reverse	CCACGTCGGAGTTTTGAGTT
FDFT1	Human	forward	CCTCAAGAGGTTTGGAGCAG
		reverse	TGGTGCAGTGCATTGGTTAT
COL1A1	Human	forward	GTGCTAAAGGTGCCAATGGT
		reverse	ACCAGGTTCACCGCTGTTAC
OCN	Human	forward	GGCGCTACCTGTATCAATGG
		reverse	TCAGCCAACTCGTCACAGTC
HPRT	Human	forward	TGGCGTCGTGATTAGTGATG
		reverse	CGAGCAAGACGTTCAGTCCT

AKR1C3 = aldo-keto reductase family 1 member C3.
ALDH3A2 = aldehyde dehydrogenase 3 family member A2.
AKR1C1 = aldo-keto reductase family 1 member C1.
SDC3 = syndecan 3, FDPS = farnesyl pyrophosphate synthetase.
GGPS1 = geranylgeranyl diphosphate synthase 1.
FDFT1 = farnesyl diphosphate farnesyltransferase 1.
COL1A1 = collagen type I alpha 1 chain, OCN = osteocalcin.
HPRT = hypoxanthine phosphoribosyltransferase 1.

(FDFT1) (13128-1-AP, Proteintech, Rosemont, IL, final concentration 10 μg/mL), rabbit anti-farnesyl pyrophosphate synthetase (FDPS) (16129-1-AP, Proteintech, final concentration 10 μg/mL), and rabbit anti-geranylgeranyl diphosphate synthase 1 (GGPS1) (14944-1-AP, Proteintech, final concentration 10 μg/mL) at 4 °C overnight. Immunofluorescent signals were observed using a fluorescence microscope (BZ-X710; Keyence, Osaka, Japan).

Clinical sample preparation

Clinical samples were prepared as previously described with the approval of the Ethics Committee of Tohoku University Graduate School of Dentistry (approval number: 2020-3-045).[9]

Statistical analysis

Statistical analysis was performed using a one-way analysis of variance, followed by Tukey's test (Fig. 2) and Dunnett's test (Fig. 3).

Results

Rosiglitazone accelerates periodontal tissue regeneration after ligature removal

To investigate whether TZDs such as rosiglitazone and troglitazone can induce periodontal tissue regeneration *in vivo*, ligature ties surrounding the second molar were removed after 14 days. Subsequently, rosiglitazone was administered locally every alternate day for 14 days. Quantitative analysis of the distance between the cemento-enamel junction and the alveolar bone crest showed that the distance was significantly narrower in the rosiglitazone-treated group than in the solvent-treated group ($P = 0.0496$), indicating that rosiglitazone administration accelerated alveolar bone regeneration (Fig. 1A). No apparent effect was observed on the non-ligature side (Fig. 1A). Masson's trichrome staining of ligated second molars that exhibited median values of the distance between the cemento-enamel junction and the alveolar bone crest in the rosiglitazone and solvent-treated control groups showed that rosiglitazone treatment induced alveolar bone regeneration (Fig. 1B).

Overexpression of full-length peroxisome proliferator-activated receptor γ specifically enhances troglitazone-induced osteo/cementogenic differentiation of periodontal ligament fibroblasts

PDLF-PPARγ, PDLF-PPARγ-UBI, PDLF-PPARγ-PDL, and PDLF-empty, which stably expressed the empty vector, were cultured in osteo/cementogenic induction medium in the presence or absence of troglitazone (10 μM) for 12 days. ALP activity and calcium nodule formation, which are specific markers of osteo/cementogenic differentiation, were evaluated every three days. PDLF-PPARγ caused a marked increase in ALP activity upon troglitazone treatment on day 6 (Fig. 2A). Concomitantly, troglitazone treatment of PDLF-PPARγ showed strong calcium nodule formation at days 9 and 12 (Fig. 2B) Therefore, analyses of the distinct isoforms revealed that the agonistic actions of troglitazone for osteo/cementogenic differentiation were caused by the full-length PPARγ isoform.

Intermediates of the isoprenoid metabolic process regulate the osteo/cementogenic abilities of periodontal ligament fibroblasts

To explore the key energy metabolic pathways associated with the osteo/cementogenic abilities of PDLFs, differentially downregulated genes of PDLFs transfected with siRNA for *PPARG* by comparing with PDLFs transfected with control siRNA were extracted from publicly available RNA-seq datasets. Subsequently, gene ontology analysis was conducted to rank the pathways suppressed by *PPARG* knockdown (Supplemental Fig. 1). Pathways associated with osteo/cementogenic differentiation and bone matrix mineralization, and with metabolic pathways are highlighted in blue and red, respectively (Fig. 3A). The isoprenoid metabolic process ranked first among the metabolic pathways. To assess whether TZD treatment upregulated the expression of isoprenoid metabolic process-related genes with high values of fragments per kilobase of exon per million mapped reads and significantly suppressed the expression level by *PPARG* knockdown, PDLFs were stimulated with TZDs for 3 and 6 days under osteo/cementogenic induction. We found that three of the four examined genes, *aldo-keto reductase family 1 member C3* (*AKR1C3*), *aldo-keto reductase family 1 member C1* (*AKR1C1*), and *syndecan 3* (*SDC3*), were upregulated by TZDs (Fig. 3B). These results indicate that TZDs were at least partially able to trigger an isoprenoid pathway in an osteogenic environment. Next, PDLFs were stimulated with the key isoprenoid intermediates FPP (20 μM) or GGPP (20 μM) for 6 days, and ALP activity was assessed (Fig. 3C). FPP increased ALP activity. However, GGPP synthesized from FPP by GGPS1 did not enhance ALP activity. TZD treatment enhanced the ALP activity of PDLFs compared to DMSO treatment, as expected, and FPP, but not GGPP, increased ALP activity. Alizarin Red S staining showed that FPP treatment accelerated calcified nodule formation (Fig. 3D). Subsequently, the expression of three catalytic enzymes in mouse periodontal ligament tissues was analyzed: FDPS, which catalyzes the production of FPP from IPP and DMAPP; GGPS1; and FDFT1, which enzymatically converts FPP to squalene. Immunohistochemical analysis of the one-third apex of the periodontal tissue of the first and second molars showed that FDPS, GGPS1, and FDFT1 were expressed in the periodontal ligament tissue, indicating that the isoprenoid metabolic process was active (Fig. 3E).

Farnesyl pyrophosphate synthetase expression is correlated with *osteocalcin* expression, and *farnesyl diphosphate farnesyltransferase 1* expression is strongly correlated with *collagen type I alpha 1 chain* expression in human clinical periodontal tissues

Human clinical periodontal tissue samples obtained during surgical or nonsurgical periodontal treatment, as described previously,[9] were used to examine whether a correlation

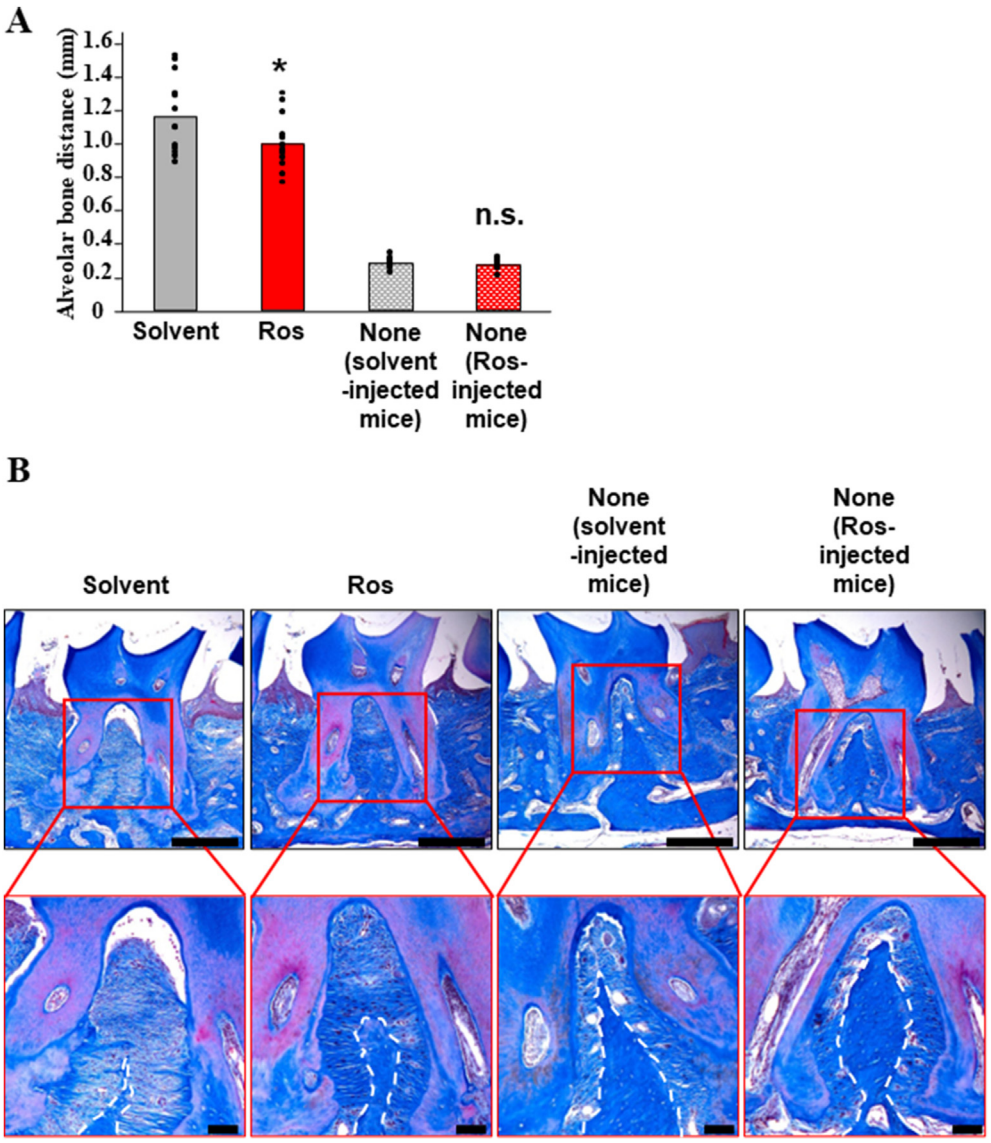

Figure 1 Local administration of rosiglitazone promotes periodontal tissue regeneration in a murine model. (A) The vertical distances from the cemento-enamel junction to the alveolar bone crest at the mesial and distal roots at 14 days after ligature removal were measured and summed (n = 13). (B) Demineralized male maxilla sections treated with 0 or 1.2 mg/kg of rosiglitazone for 14 days after ligature removal were stained with Masson's trichrome. *$P < 0.05$ was considered to be a statistically significant difference from the control. n.s. = not significant. The border of the alveolar bone and periodontal ligament tissue are indicated by dash line. Scale bars correspond to 500 and 100 μm at low and high magnification, respectively. Ros = rosiglitazone.

existed between the expression levels of *OCN*, an osteo/cementogenic-related gene; *COL1A1*, an ECM-related gene; and *FDPS*, *GGPS1*, or *FDFT1*. A weak correlation between *OCN* and *FDPS* was identified (r = 0.221); however, no apparent correlation between *OCN* and *GGPS*1 (r = 0.173) or between *OCN* and *FDFT1* (r = −0.036) was observed (Fig. 4). *COL1A1* expression was strongly correlated with *FDFT1* (r = 0.947) but not with *FDPS* (r = −0.014) or *GGPS1* (r = −0.032).

Discussion

PPARγ agonists, such as rosiglitazone and procyanidin B2, can prevent periodontal tissue breakdown in experimental periodontitis models.[9,24] The present study demonstrated for the first time that local administration of TZDs into regenerating periodontal tissue accelerated periodontal tissue regeneration in an animal model (Fig. 1). Mechanistically, the TZD-induced differentiation abilities of PDLFs relied on full-length PPARγ rather than the other two deleted isoforms (Fig. 2). Furthermore, both FPP and GGPP showed potent but inverse effects on the osteo/cementogenic abilities of PDLFs, with FPP showing inducible abilities (Fig. 3).

Among the PPARγ agonists, troglitazone showed the most drastic inducible effects on osteo/cementogenic differentiation and matrix mineralization of PDLFs *in vitro*,[8] we conducted *in vitro* experiments primarily with troglitazone as the PPARγ agonist (Fig. 2). However, troglitazone

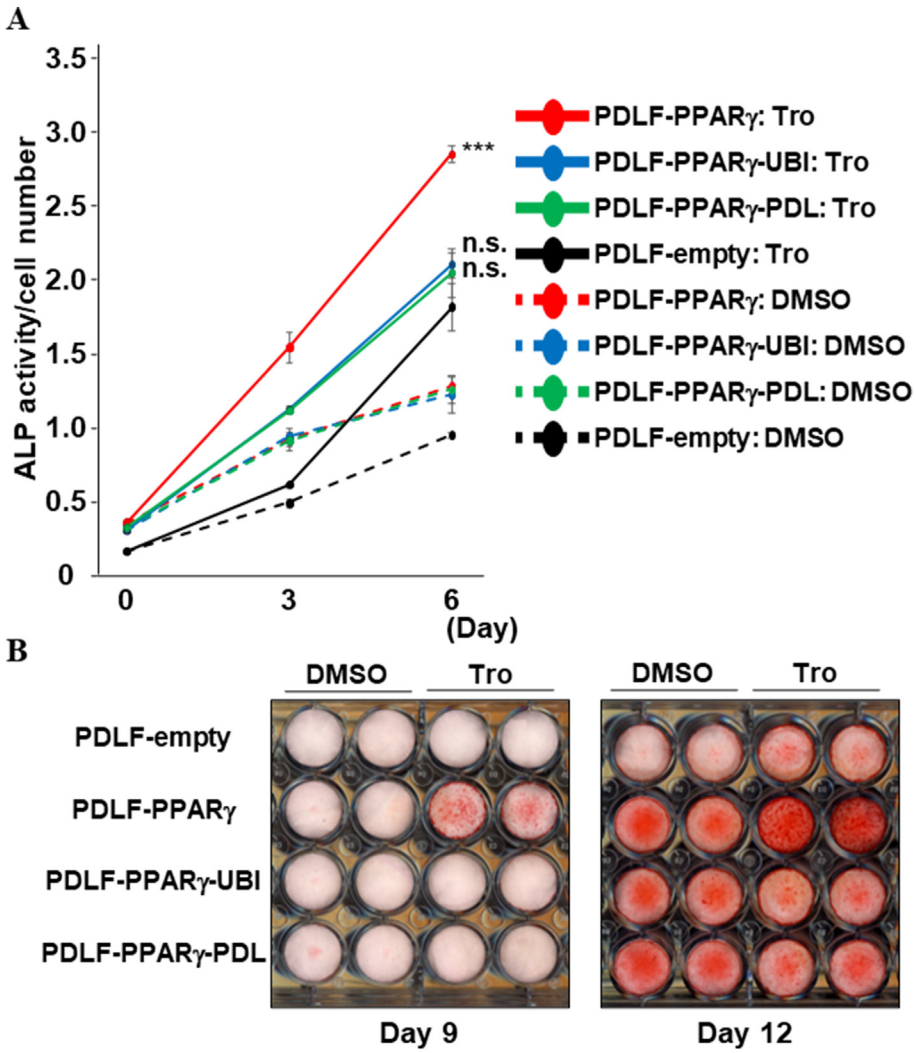

Figure 2 Overexpression of full-length PPARγ specifically enhances troglitazone-induced osteo/cementogenic differentiation of PDLFs. (A, B) PDLF-empty, PDLF-PPARγ, PDLF-PPARγ-UBI, and PDLF-PPARγ-PDL were cultured in mineralization-inducing medium for a maximum of 12 days. ALP activities were normalized by cell numbers (A) and calcium deposition was visualized by Alizarin Red S staining (B). ***$P < 0.001$ was considered a statistically significant difference compared with the PDLF-empty treated with troglitazone on day 6. n.s. = not significant, Tro = troglitazone.

was replaced with rosiglitazone for clinical use as a drug for type 2 diabetes mellitus because of its hepatotoxicity.[25–27] Therefore, rosiglitazone was used for the *in vivo* study (Fig. 1). As the original ALP activities (day 0) and the ALP activities at the early differentiation stage (day 3) of PDLF-PPARγ, PDLF-PPARγ-UBI, and PDLF-PPARγ-PDL were higher than those of PDLF-empty (Fig. 2A). Not only full-length PPARγ, but PPARγ-UBI and PPARγ-PDL possessed osteo/cementogenic inducible abilities independent of TZDs. In particular, *PPARγ-PDL* expression in clinical periodontal tissue was highly correlated with *COL1A1* expression.[9] The deduced amino acid sequence indicates that PPARγ-UBI and PPARγ-PDL lack the ligand binding domain. Therefore, PPARγ-UBI and PPARγ-PDL may not act as a nuclear receptor. Some portions of the overexpressed PPARγ-UBI and PPARγ-PDL localized in the cytoplasm. Further studies are required to determine how PPARγ-UBI and PPARγ-PDL enhance osteo/cementogenic abilities by modulating protein-protein interactions in PDLFs.

Acetyl-CoA participates in lipid, glucose, and amino acid metabolism and is the starting material for the mevalonate pathway.[28] Amino-bisphosphonate, an analog of inorganic pyrophosphate, which inhibits FDPS enzymatic ability in osteoclasts, protects against osteoporosis.[29–31] Thus, inhibition of the mevalonate pathway can retain bone volume and bone mineral density *in vivo*. In contrast, the *in vitro* finding that FPP accelerated the osteo/cementogenic differentiation and matrix mineralization abilities of PDLFs suggested a preferable role of FPP in PDLFs (Fig. 3). In line with the present study, PDLFs stimulated with alendronate, an amino-bisphosphonate, at physiological concentrations (2–25 μM) showed lower ALP activity and suppressed calcified nodule formation.[32] As FPP showed preferential but GGPP showed adverse effects (Fig. 3), *FDPS* expression was more correlated with *OCN* than *GGPS1* and *FDFT1* (Fig. 4), and the expression levels of *COL1A1* and *FDFT1* were highly correlated (Fig. 4), selective conversion of FPP into squalene rather than GGPP might be key for FPP-

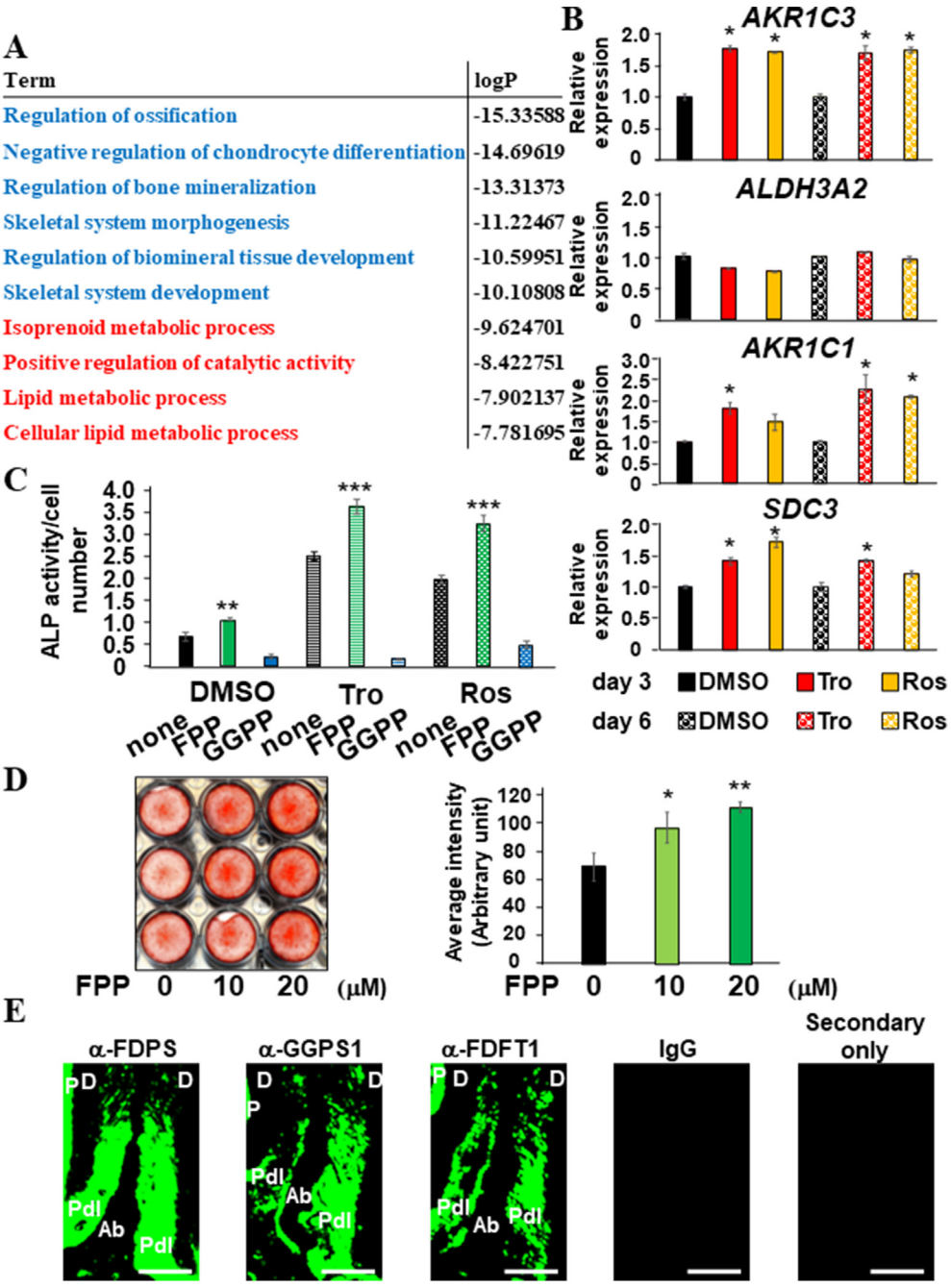

Figure 3 The isoprenoid metabolic process is most severely downregulated metabolic pathway in PPARγ-knockdown PDLFs. (A) Gene ontology analysis of the downregulated genes in PDLFs transfected with siRNA for PPARG by comparing with PDLFs transfected with control siRNA. Raw RNA-seq data were obtained from NCBI's Gene Expression Omnibus (GEO) under accession number GSE178607. (B) PDLF-1 cells were cultured in mineralization-inducing medium for 3 and 6 days in the presence of troglitazone (10 μM) or rosiglitazone (10 μM). The gene expression levels of *AKR1C3*, *ALDH3A2*, *AKR1C1*, and *SDC3*, which were categorized in "isoprenoid metabolic process" and identified as the downregulated genes in PPARG-knockdown PDLFs, were evaluated. (C) PDLFs were cultured in mineralization-inducing medium for 6 days in the presence of troglitazone (10 μM) or rosiglitazone (10 μM) and FPP (20 μM) or GGPP (20 μM). ALP activities were normalized by cell numbers. (D) PDLFs were cultured in mineralization-inducing medium for 12 days in the presence of FPP (0, 10, 20 μM), and calcium deposition was visualized and quantified by Alizarin Red S staining. (E) Demineralized 1.5-month-old maxilla sections were stained without the primary antibody or with mouse IgG, α-FDPS, α-GGPS1, or α-FDFT1 antibodies, $^{*}P < 0.05$; $^{**}P < 0.01$; $^{***}P < 0.001$ indicated significantly higher expression levels compared with those in DMSO-treated PDLFs at each day point (B), non-treated PDLFs in either DMSO, troglitazone, or rosiglitazone treatment group (C), and non-treated PDLFs (D). Tro = troglitazone. Ros = rosiglitazone. P = pulp. D = dentin. Pdl = periodontal ligament tissue. Ab = alveolar bone. Scale bars correspond to 100 μm.

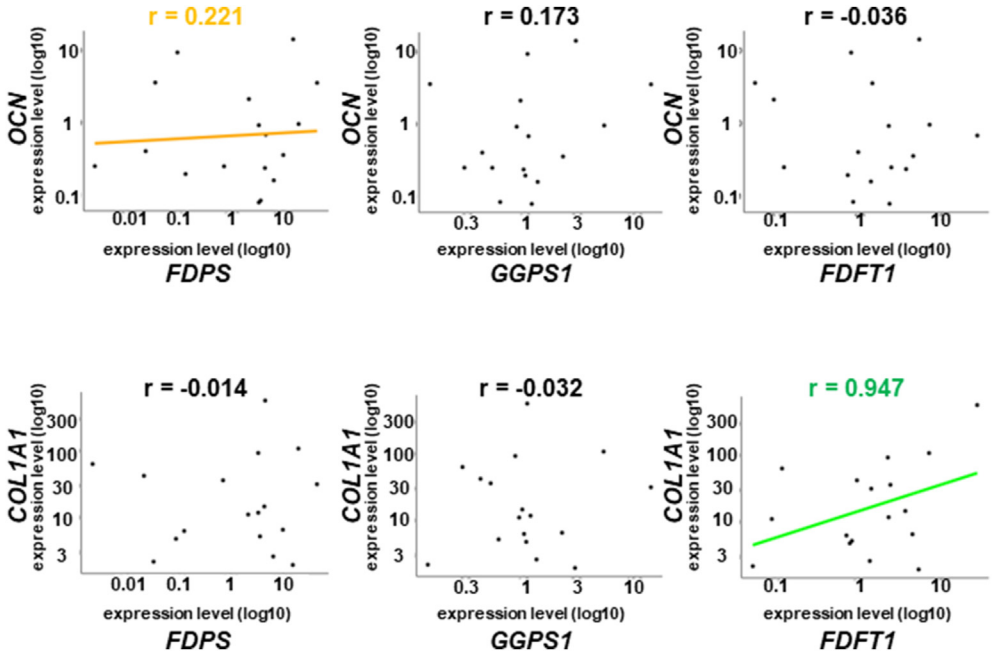

Figure 4 Correlation between *OCN* or *COL1A1* and *FDPS*, *GGPS1*, or *FDFT1* expression in human clinical periodontal tissue. Human clinical periodontal tissues (18 samples from different patients) were collected, and the correlative expression levels of *OCN* or *COL1A1* with *FDPS*, *GGPS1*, or *FDFT1* were examined. The high ($r > 0.8$ or $r < -0.8$) and weak correlations ($0.2 < r < 0.4$ or $-0.4 < r < -0.2$) are indicated by green and orange lines, respectively.

induced matrix mineralization and differentiation of PDLFs (Fig. 3D). Further studies are necessary to investigate the precise molecular mechanisms by which exogenous FPP and its derived intermediates participate in the osteo/cementogenic differentiation and matrix mineralization of PDLFs.

In conclusion, by applying a PPARγ agonist to a murine periodontal regeneration model and utilizing PDLFs expressing various isoforms of PPARγ, we found that PPARγ agonistic actions facilitated periodontal tissue regeneration by specifically activating the most abundant isoform, full-length PPARγ. FPP, but not GGPP, induced osteo/cementogenic differentiation of PDLFs. Thus, in addition to the local application of TZDs and FPP, precise control of the activities of FDPS, GGPS1, and FDFT1 in periodontal ligament tissue could be a novel therapeutic method for periodontal regeneration.

Declaration of competing interest

The authors have no conflicts of interest relevant to this article.

Acknowledgments

This study was financially supported by JSPS KAKENHI Grant Numbers 22H03266 and 22K19611 to Shigeki Suzuki and 23H03077 and 23K18350 to Satoru Yamada. We would like to thank Editage (www.editage.jp) for English language editing.

Appendix A. Supplementary data

Supplementary data to this article can be found online at https://doi.org/10.1016/j.jds.2024.04.025.

References

1.. Chang YT, Lai CH, Yu JH, et al. Exploring the impact of culture techniques and patient demographics on the success rate of primary culture of human periodontal ligament stem cells. *J Dent Sci* 2024;19:961—70.
2. Yang Y, Alves T, Miao MZ, et al. Single-cell transcriptomic analysis of dental pulp and periodontal ligament stem cells. *J Dent Res* 2024;103:71—80.
3. Manokawinchoke J, Chareonvit S, Trachoo V, Limraksasin P, Egusa H, Osathanon T. Intermittent compressive force regulates dentin matrix protein 1 expression in human periodontal ligament stem cells. *J Dent Sci* 2023;18:105—11.
4. Iwayama T, Iwashita M, Miyashita K, et al. Plap-1 lineage tracing and single-cell transcriptomics reveal cellular dynamics in the periodontal ligament. *Development* 2022;149: dev201203.
5. Lee S, Chen D, Park M, et al. Single-cell RNA sequencing analysis of human dental pulp stem cell and human periodontal ligament stem cell. *J Endod* 2022;48:240—8.
6. Lim WH, Liu B, Cheng D, Williams BO, Mah SJ, Helms JA. Wnt signaling regulates homeostasis of the periodontal ligament. *J Periodontal Res* 2014;49:751—9.
7. Nagayasu-Tanaka T, Anzai J, Takaki S, et al. Action mechanism of fibroblast growth factor-2 (FGF-2) in the promotion of periodontal regeneration in beagle dogs. *PLoS One* 2015;10: e0131870.
8. Yuan H, Suzuki S, Hirata-Tsuchiya S, et al. PPARγ-induced global H3K27 acetylation maintains osteo/cementogenic abilities of periodontal ligament fibroblasts. *Int J Mol Sci* 2021;22: 8646.
9. Yamamoto T, Yuan H, Suzuki S, Nemoto E, Saito M, Yamada S. Procyanidin B2 enhances anti-inflammatory responses of periodontal ligament cells by inhibiting the dominant negative pro-inflammatory isoforms of peroxisome proliferator-activated receptor. *J Dent Sci* 2024;19:1801—10.

10. Aprile M, Cataldi S, Ambrosio MR, et al. PPARγΔ5, a naturally occurring dominant-negative splice isoform, impairs PPARγ function and adipocyte differentiation. *Cell Rep* 2018;25:1577—92.
11. Ahmadian M, Suh JM, Hah N, et al. PPARγ signaling and metabolism: the good, the bad and the future. *Nat Med* 2013;19:557—66.
12. Shi L, Tu BP. Acetyl-CoA and the regulation of metabolism: mechanisms and consequences. *Curr Opin Cell Biol* 2015;33:125—31.
13. Sato A, Suzuki S, Yuan H, et al. Pharmacological activation of YAP/TAZ by targeting LATS1/2 enhances periodontal tissue regeneration in a murine model. *Int J Mol Sci* 2023;24:970.
14. Tao S, Yang T, Zhou JN, Zhang Q. Impaired pulp healing associated with underlying disorders in the dental pulp of rats with type 2 diabetes. *J Dent Sci* 2024;19:310—20.
15. Luo C, He J, Wang N, et al. Enhanced reparatory effect of EI1 on dental pulp via extracellular matrix remodeling by miR-181b-2-3p inhibitor. *J Dent Sci* 2024;19:177—85.
16. Jaha H, Husein D, Ohyama Y, et al. N-terminal dentin sialoprotein fragment induces type I collagen production and upregulates dentinogenesis marker expression in osteoblasts. *Biochem Biophys Rep* 2016;6:190—6.
17. Yuan H, Suzuki S, Terui H, et al. Loss of IκBζ drives dentin formation via altered H3K4me3 status. *J Dent Res* 2022;101:951—61.
18. Yoshida K, Suzuki S, Kawada-Matsuo M, et al. Heparin-LL37 complexes are less cytotoxic for human dental pulp cells and have undiminished antimicrobial and LPS-neutralizing abilities. *Int Endod J* 2019;52:1327—43.
19. Suzuki S, Sasaki K, Fahreza RR, Nemoto E, Yamada S. The histone deacetylase inhibitor MS-275 enhances the matrix mineralization of dental pulp stem cells by inducing fibronectin expression. *J Dent Sci* 2024;19:1680—90.
20. Yoshida K, Suzuki S, Yuan H, et al. Public RNA-seq data-based identification and functional analyses reveal that MXRA5 retains proliferative and migratory abilities of dental pulp stem cells. *Sci Rep* 2023;13:15574.
21. Suzuki S, Yuan H, Hirata-Tsuchiya S, et al. DMP-1 promoter-associated antisense strand non-coding RNA, panRNA-DMP-1, physically associates with EGFR to repress EGF-induced squamous cell carcinoma migration. *Mol Cell Biochem* 2021;476:1673—90.
22. Suzuki S, Fukuda T, Nagayasu S, et al. Dental pulp cell-derived powerful inducer of TNF-α comprises PKR containing stress granule rich microvesicles. *Sci Rep* 2019;9:3825.
23. Suzuki S, Hoshino H, Yoshida K, et al. Genome-wide identification of chromatin-enriched RNA reveals that unspliced dentin matrix protein-1 mRNA regulates cell proliferation in squamous cell carcinoma. *Biochem Biophys Res Commun* 2018;495:2303—9.
24. Hassumi MY, Silva-Filho VJ, Campos-Júnior JC, et al. PPAR-gamma agonist rosiglitazone prevents inflammatory periodontal bone loss by inhibiting osteoclastogenesis. *Int Immunopharmacol* 2009;9:1150—8.
25. Smith MT. Mechanisms of troglitazone hepatotoxicity. *Chem Res Toxicol* 2003;16:679—87.
26. Yokoi T. Troglitazone. *Handb Exp Pharmacol* 2010;196:419—35.
27. Kores K, Konc J, Bren U. Mechanistic insights into side effects of troglitazone and rosiglitazone using a novel inverse molecular docking protocol. *Pharmaceutics* 2021;13:315.
28. Miziorko HM. Enzymes of the mevalonate pathway of isoprenoid biosynthesis. *Arch Biochem Biophys* 2011;505:131—43.
29. McClung M, Harris ST, Miller PD, et al. Bisphosphonate therapy for osteoporosis: benefits, risks, and drug holiday. *Am J Med* 2013;126:13—20.
30. Russell RGG, Watts NB, Ebetino FH, Rogers MJ. Mechanisms of action of bisphosphonates: similarities and differences and their potential influence on clinical efficacy. *Osteoporos Int* 2008;19:733—59.
31. Amin D, Cornell SA, Gustafson SK, et al. Bisphosphonates used for the treatment of bone disorders inhibit squalene synthase and cholesterol biosynthesis. *J Lipid Res* 1992;33:1657—63.
32. Vito AD, Chiarella E, Sovereto J, et al. Novel insights into the pharmacological modulation of human periodontal ligament stem cells by the amino-bisphosphonate Alendronate. *Eur J Cell Biol* 2023;102:151354.